Solar Energy
And Sustainable Development
Refereed, biannual scientific journal issued by:
The Libyan Center for Solar Energy Research and Studies

First-Principles Study of Ge-Doped $CH_3NH_3PbI_3$ Perovskite: Optical and Electronic Properties

Lhouceine Moulaoui[1*], Abdelhafid Najim[2], Abdelmounaim Laassouli[3], Omar Bajjou[4], Khalid Rahmani[5], Bouzid Manaut[6].

[1,6]LRPSI, Faculty of Polydisciplinary, Sultan Moulay Slimane University, Beni Mellal-Morocco.
[2,3,4]Laboratory of Engineering in Chemistry and Physics of Matter (LIPCM), Faculty of Sciences and Technics, Sultan Moulay Slimane University, Beni Mellal, Morocco.
[4]UNESCO UNISA Africa Chair in Nanosciences & Nanotechnology (U2ACN2), College of Graduate Studies, University of South Africa (UNISA), Pretoria, South Africa.
[5]PSES, ERC, Ecole Normale Supérieure, Mohammed V University in Rabat, Takkadoum Rabat-10000, Morocco.

E-*mail:* [1] moulaoui.h.fpbm@gmail.com .

SPECIAL ISSUE ON:

The 1St International Conference on Sciences and Techniques for Renewable Energy and the Environment.
(STR2E 2025)
May 6-8, 2025 at FST-Al Hoceima- Morocco.

KEYWORDS

$CH_3NH_3PbI_3$, Absorption coefficient, Bandgap energy, Density of states, Refractive index.

ABSTRACT

This study focuses on the examination of the optical and electronic properties of CH_3 NH_3 PbI_3 perovskite structures, with particular emphasis on the effect of germanium (Ge) doping on these properties. The aim of this study is to explore how doping CH_3NH_3 PbI_3 with Ge can affect its optoelectronic properties and thus optimize its efficiency in applications such as photovoltaic solar cells. We used the code CASTEP from the Materials Studio software to calculate the optical and electronic attributes of perovskite structures $CH_3NH_3PbI_3$, doping the lead (Pb) metal with three different percentages of germanium: 12.5%, 25%, and 37.5%. Pure $CH_3NH_3PbI_3$ perovskite has a bandgap energy (Eg) of 1.733 eV. The bandgap energies of the doped materials are 1.57 eV, 1.545 eV, and 1.503 eV, respectively. The pure $CH_3NH_3PbI_3$ structure has a maximum absorption coefficient of $8{,}11x10^{-4}$ cm^{-1} in the wavelength range of 400 nm to 800 nm. This calculation also studied the effects of Ge doping on the bandgap energy, absorption, total density of states, the real and imaginary components of the dielectric function, as well as the refractive index, the optical conductivity, and the loss function. The computed results align with the experimental findings and provide information on the possibility of modulating the optical properties and electronic of $CH_3NH_3PbI_3$ through Ge doping, doping $CH_3NH_3PbI_3$ with Ge enhances its optoelectronic properties, particularly its

*Corresponding author.

DOI: https://doi.org/10.51646/jsesd.v14iSTR2E.799

absorption in the visible range, optimizing its efficiency in photovoltaic solar cells. These improvements make Ge-doped $CH_3NH_3PbI_3$ promising for renewable energy applications, as well as in light-emitting diodes and laser devices.

دراسة من المبادئ الأولى للبيروفسكايت $CH_3\ NH_3\ PbI_3$ المطعَّم بالجرمانيوم: الخصائص البصرية والإلكترونية

الحسين مولاوي، عبد الحافظ نجيم، عبد المنعم العسولي ، عمر باجو، خالد الرحماني، بوزيد مانوط.

ملخص: تركز هذه الدراسة على فحص الخصائص البصرية والإلكترونية لهياكل البيروفسكايت $CH_3\ NH_3\ PbI_3$، مع التركيز بشكل خاص على تأثير تطعيمها بالجرمانيوم (Ge) على هذه الخصائص. تهدف هذه الدراسة إلى استكشاف كيفية تأثير تطعيم $CH_3\ NH_3\ PbI_3$ بالجرمانيوم على خصائصه البصرية والإلكترونية، مما يساعد في تحسين كفاءته في تطبيقات مثل الخلايا الشمسية الكهروضوئية. استخدمنا شفرة CASTEP من برنامج Materials Studio لحساب الخصائص البصرية والإلكترونية لهياكل البيروفسكايت $CH_3\ NH_3\ PbI_3$ ، حيث تم استبدال معدن الرصاص (Pb) بثلاث نسب مختلفة من الجرمانيوم 2.5 1 %، 25 %، و 37.5 % . يتمتع البيروفسكايت النقي $CH_3\ NH_3\ PbI_3$ بطاقة فجوة نطاق (Eg) قدرها 1.733 eV، في حين أن قيم فجوة النطاق للمواد المطعمة هي 1.57 eV، 1.545eV ، 1.503eV، على التوالي. تمتلك البنية النقية لـ $CH_3\ NH_3\ PbI_3$ معامل امتصاص أقصى يبلغ $8{,}11x10^{-4}\ cm^{-1}$ ضمن نطاق الطول الموجي بين 400 nm و 800nm. كما تناولت هذه الدراسة تأثيرات تطعيم الجرمانيوم على طاقة فجوة النطاق، الامتصاص، الكثافة الكلية لحالات الطاقة، المكونات الحقيقية والتخيلية للدالة العازلة، معامل الانكسار، التوصيلية البصرية، ودالة الفقد البصري. تتوافق النتائج المحسوبة مع النتائج التجريبية، مما يوفر معلومات حول إمكانية تعديل الخصائص البصرية والإلكترونية لـ $CH_3\ NH_3\ PbI_3$ من خلال تطعيمه بالجرمانيوم. يساهم تطعيم $CH_3\ NH_3\ PbI_3$ بالجرمانيوم في تحسين خصائصه البصرية والإلكترونية، خاصةً قدرته على الامتصاص في نطاق الضوء المرئي، مما يعزز كفاءته في الخلايا الشمسية الكهروضوئية. تجعل هذه التحسينات بيروفسكايت $CH_3\ NH_3\ PbI_3$ المطعم بالجرمانيوم مادة واعدة لتطبيقات الطاقة المتجددة، بالإضافة إلى استخدامه في الثنائيات الباعثة للضوء (LEDs) وأجهزة الليزر.

الكلمات المفتاحية: $CH_3NH_3PbI_3$؛ معامل الامتصاص، طاقة فجوة النطاق، كثافة حالات الطاقة، معامل الانكسار.

1. INTRODUCTION

Energy consumption is rising sharply due to the rapid growth of the global population and the expansion of industrial units [1]. This situation not only exacerbates the energy shortage but also worsens environmental pollution. Therefore, it has become imperative and it is crucial to discover new sources of sustainable and clean energy. In this context, solar energy possesses now emerged as one of the leading options [2-5].

Photovoltaic energy is a form of renewable energy that generates no pollution, utilizing solar cells to capture and convert light rays into electricity. Currently, innovative research is focusing on metal halide perovskites with a general formula of ABX_3 [6]. In this formula, A^+ refers to the organic ion $CH_3\ NH_3^+$ (MA^+), B^{2+}, corresponds to Pb^{2+}, where X^-denotes a halide ion such as I^-, Cl^-, or Br^-. These types of perovskites are known for their outstanding optical and electronic properties, which hold significant promise for solar technology applications. In the year 2009, Kojima and his team successfully used 3D perovskite $MAPbI_3$ in combination with a liquid electrolyte in solar cells, achieving a 3.8% efficiency More recently, in 2012, Other rese arch substituted the liquid electrolyte with a solid one, achieving an efficiency of 9% [7]. Our research is centered on a detailed analysis of characteristics of organometallic methylammonium lead triiodide perovskite $CH_3\ NH_3\ PbI_3$.

The use of perovskites in photovoltaic technology has seen significant advancements over the past decade, with recently certified power conversion efficiencies surpassing 25.2% [8]. However, all perovskites that have achieved such high efficiencies to date contain lead. As a result, there has been growing interest in lead-free perovskites made from alternative metals, such as germanium (Ge). Although germanium-based perovskites are still relatively underexplored, it is expected that interest in these materials will increase in the coming years, driven by their potential for a wide range of applications. Ge is an abundant metal, and when compared to lead, it offers lower toxicity and fewer environmental concerns [9]. However, additional research is still required to fully explore the broad potential applications of germanium-based perovskite cells.

Doping perovskite materials with Ge significantly boosts their performance in photovoltaic applications. It enables precise control over the band gap, enhancing light absorption and overall efficiency. Germanium-based perovskites also demonstrate greater stability, particularly against environmental challenges such as moisture and UV radiation, while offering lower toxicity compared to conventional lead-based perovskites, making them a more sustainable option. Furthermore, Ge doping helps reduce charge carrier recombination, improving charge transport and increasing power conversion efficiency. These advantages make germanium-doped perovskites a promising alternative for high-performance, environmentally friendly solar cells. In recent years, $MAPbI_3$ perovskite has become extensively utilized as an effective photovoltaic absorption layer, thanks to its considerable gains [10]. These include a high absorption, an optimal bandgap energy, notable photoelectric conversion efficiency [11]. Three distinct crystal structures are observed in $MAPbI_3$: $MAPbI_3$ has an orthorhombic phase with P221 space group at temperatures below 162.2 K, a tetragonal phase with the space group I4/mcm between 162 K and 327.4 K, and a cubic phase with the Pm3m space group at temperatures exceeding 327.4 K[12].

This study focused on analyzing the optoelectronic characteristics of pure $MAPbI_3$ and examined the impact of doping with Ge on these properties. Specifically, we introduced Ge atoms into the Pb sites at doping levels of 12.5%, 25%, and 37.5%.

2. COMPUTATIONAL PROCEDURES

Optical and elctronic characteristics attributes of $MAPbI_3$ were analyzed using Density Functional Theory (DFT). These properties were computed employing the Cambridge Sequential Total Energy Program (CASTEP) [13,14]. In the $MAPbI_3$ structure, to ensure precise calculations, ultrasoft pseudopotentials were utilized for representing the electrons of valence, using functional of Perdew-Burke-Ernzerhof (PBE) and the generalized gradient approximation (GGA) [15]. Electron-ion interactions were characterized through the OTFG ultrasoft pseudopotential [16,17]. Optimizing the geometry of the materials was essential for attaining stable configurations of the relaxed structures, necessitating stringent convergence criteria for both atomic positions and lattice parameters. A energy cut-off of 500 eV was used for calculations. The Brillouin zone was sampled using K points arranged in a 5×5×1. For the self-consistent field operations, the Pulay density mixing method was used, adopting a convergence criterion of $2x10^{-6}$ eV/atom [12]. The maximum allowable stress was 0.1 GPa. The valence shell configurations of the atoms considered are: H: 1s1, C: $2s^22p^2$, N: $2s^22p^3$, Ge: $4s^24p^2$, Pb: $6s^2$, and I: $5s^25p^5$. A 2×1×1 supercell of $MAPbI_3$ tetragonal was the focus of this study, with lattice dimensions of a = b = 8.851 Å, c = 12.642 Å and $\alpha = \beta = \gamma = 90°$ The lattice dimensions adopted in this study, namely a = b = 8.851 Å and c = 12.642 Å, were extracted from experimental studies [12] . These values have been validated and serve as the basis for our calculations and analyses. Figure 1 illustrates the tetragonal structure of $MAPbI_3$ and its germanium-doped variants, the bond lengths of the atoms in the $MAPbI_3$ perovskite are presented in the table 1 below. These values may vary slightly depending on the crystal phase and

experimental conditions.

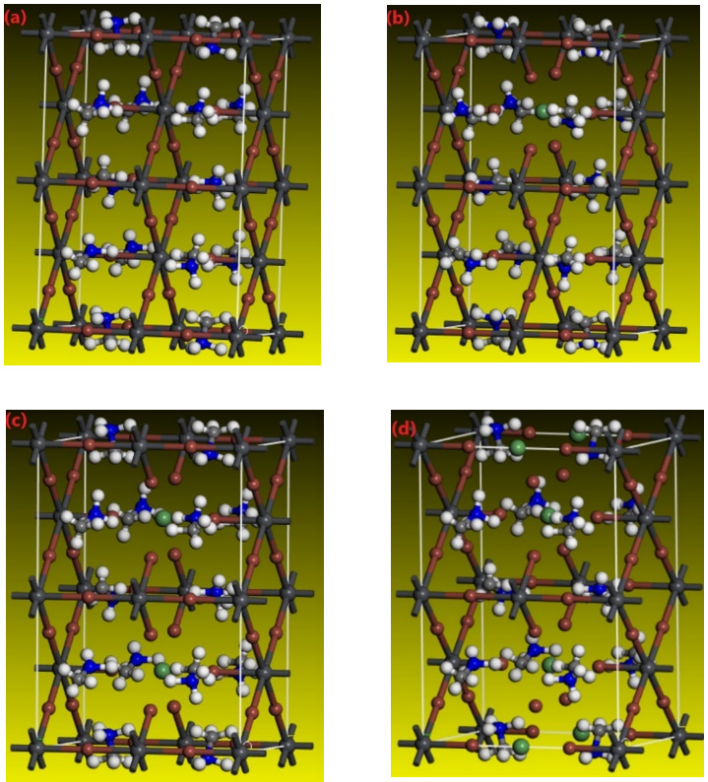

Fig.1.Tetragonal structures of $CH_3NH_3PbI_3$, showing (a) pure $MAPbI_3$, (b) $MAPb_{0.85}Ge_{0.125}PbI_3$, (c) $MAPb_{0.75}Ge_{0.25}PbI_3$, and (d) $MAPb_{0.625}Ge_{0.375}PbI_3$, with color codes: black (C), white (H), blue (N), bluish-gray (Pb), dark gray (I) and green (Ge).

Table 1 . Bond lengths of the atoms in the $MAPbI_3$.

Bands	Length (Å)
Pb-I	3.2
N–H	1.03
C–H	1.09
C–N	1.42

3. FINDINGS AND EVALUATION

3.1. Electronic structure

3.1.1. Band gap

A material's photoelectric properties and band structure are essential factors influencing the efficiency of photovoltaic conversion in solar cells. We calculated the bandgap energy for $CH_3NH_3PbI_3$, and its germanium-doped variants $MAPb_{1-x}Ge_xPbI_3$ with x values of 0.125, 0.25, and 0.375 along the high-symmetry directions as illustrated in Figure 2. The results show that $MAPbI_3$ functions as a semiconductor characterized by a direct bandgap, with an enegy of 1.733 eV. For the doped structures, the bandgap energies are 1.57 eV for x = 0.125, 1.545 eV for x = 0.25 and 1.503 eV for x = 0.375. These findings confirm that all these structures are made up of semiconductor materials. The conduction band's lowest energy point and the highest energy point of the valence band both take place at the G point in the Brillouin zone. These findings

suggest that varying the germanium doping concentration affects the bandgap of the $MAPbI_3$ perovskite. In summary, the decrease in the bandgap energy observed when doping germanium into $MAPbI_3$ results from perturbations in the crystal lattice structure and associated energy levels. These disturbances alter the electronic properties of the material, leading to a reduction in the bandgap width.

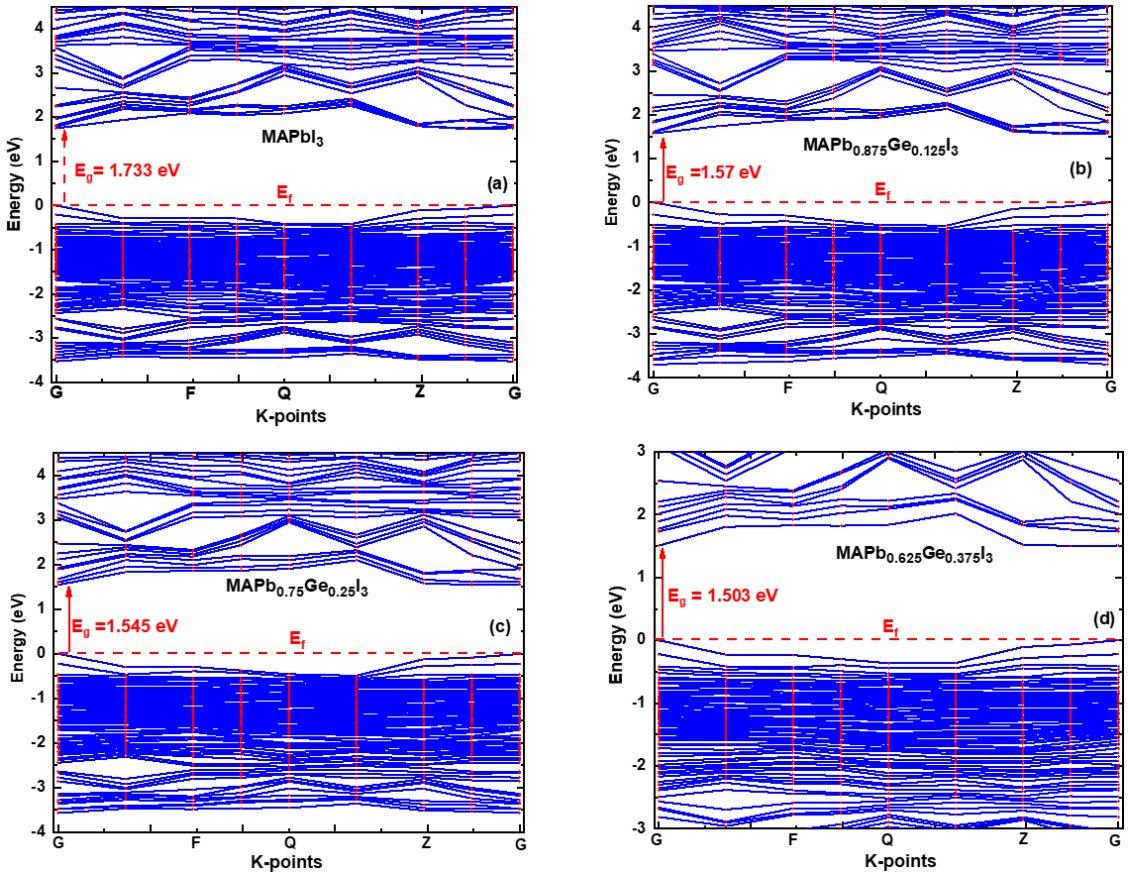

Fig. 2. Energy band of pure and doped $MAPbI_3$, (a) pure structure, (b) $MAPb_{0.85}Ge_{0.125}PbI_3$, structure, (c) $MAPb0.75\ Ge_{0.25}\ PbI_3$ structure (d) $MAPb_{0.625}\ Ge_{0.375}\ PbI_3$.

Doping the $MAPbI_3$ perovskite with Ge decreases the bandgap [18]. These results are consistent with other previously published findings. The table 1 below presents the bandgap obtained in our calculation along with those from other calculations using different approximations.

Table 2 : Comparison of the Bandgap (Eg) of $MAPbI_3$ using different approximations.

Apprimations	**Bandgap (Eg)**
GGA-PBE	1.733 eV [This work]
GGA-PBE	1.761 [18]
HSE06	1.97 eV [19]
Experimental	1,55 eV [20]

3.1.2. Density of states

The total density of states (TDOS) plays a crucial role in defining these characteristics, which shows how Kohn-Sham eigenvalues are distributed across various occupied and unoccupied orbitals. The bandgap energy is indicated by the contrast between states in the upper valence band (VB) and those in the lower conduction band (CB). Figure 3 displays the TDOS for both

undoped $MAPbI_3$ and $MAPb_{1-x}Ge_x PbI_3$. These calculations utilized the GGA-PBE method [21]. The TDOS profiles highlight the positions of distinct peaks and illustrate the contributions of specific electronic states linked to H, C, N, Pb, I, and Ge atoms. The interaction of these states forms the perovskite. The spectra of TDOS obtained show distinct regions for the VB and a separate region for the CB. In summary, doping lead with germanium in the $MAPbI_3$ perovskite modifies the TDOS by introducing new energy levels, reconfiguring electronic states, and adjusting the intensity of peaks [22]. These changes influence the distribution of electronic states in the material and can affect its optical and electronic properties.

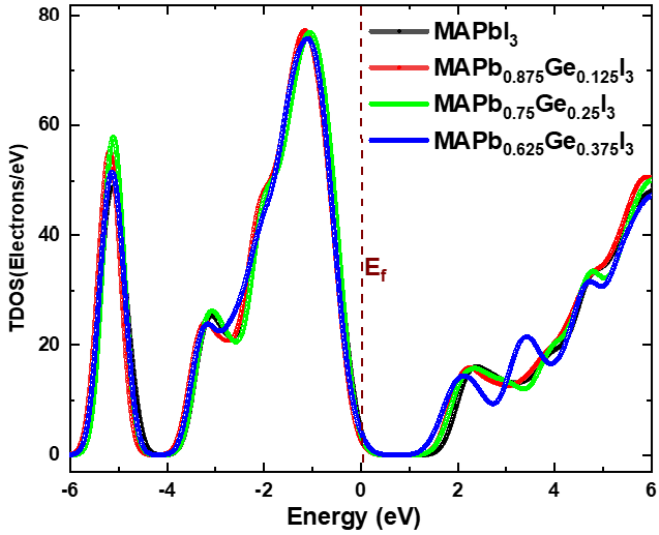

Fig. 3. TDOS for $MAPbI_3$ and $MAPb_{1-x}Ge_x PbI_3$ structures at doping ratios of x = 0.125 ; 0.25 and 0.375.

3.2. Optical characteristics

3.2.1. Absorption

The absorption is a critical parameter for assessing the performance of SC and other materials utilized in technologies associated with energy. This property indicates how effectively a material can absorb light at specific wavelengths, which directly impacts its efficiency in converting solar energy into usable power. Figure 4 displays the spectral absorption coefficients for both $MAPbI_3$ and $MAPb_{1-x}Ge_x PbI_3$. The data reveal an absorption peak within the 300 nm to 400 nm wavelength range. For the pure $MAPbI_3$ structure, this peak is situated around 350 nm, illustrating its wavelength-specific absorption characteristics, spanning both the UV and visible spectra. In the span of 300-400 nm, doping Pb with Ge in the perovskite leads to a lower level of absorption, while in the interval of 400 nm to 800 nm, doping increase the absorption coefficient, as shown in Fig.4. This variation can be attributed to several mechanisms. In the UV range 300-400 nm, germanium doping alters the perovskite's bandgap, introducing intermediate electronic states that may interfere with photon absorption in this energy range. These intermediate states can reduce the material's effectiveness in absorbing UV light. Conversely, in the visible range 400-800 nm, doping improves absorption by narrowing the bandgap, which better aligns the material's energy levels with photons in this range. Consequently, germaniun-doped perovskite exhibits enhanced absorption in the visible spectrum, which proves advantageous for photovoltaic and photonic technologies where visible light absorption is critical. Doping the $MAPbI_3$ perovskite with Ge enhances absorption in the visible range, these results are consistent with previously published studies [18].These doping-induced properties optimize the performance of solar cells by making more efficient use of incident light.

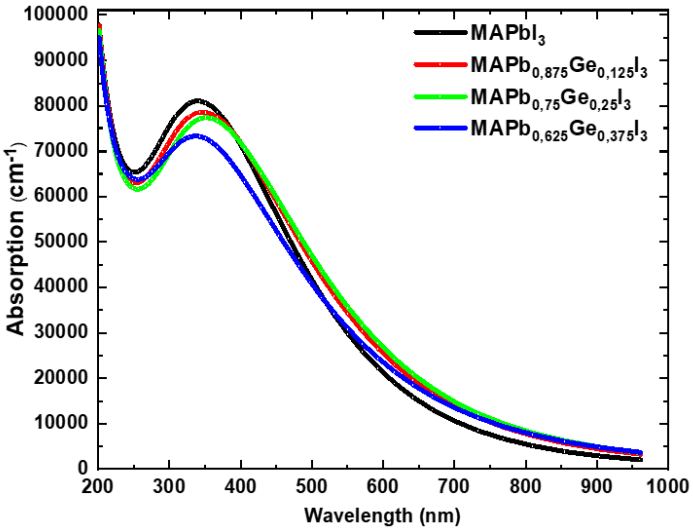

Fig. 4. Absorption of $MAPbI_3$ and $MAPb_{1-x}Ge_x$ PbI_3 materials (x = 0.125, 0.25, 0.375).

Dielectric function

The complex dielectric function provides insight into how light interacts as it propagates through a material. It distinguishes dispersion effects through its real part, $\varepsilon_1(\omega)$, and absorption effects through its imaginary part, $\varepsilon_2(\omega)$. The general expression for this relationship is given by [22].

$$\varepsilon(\omega) = \varepsilon_1(\omega) + i\varepsilon_2(\omega) \qquad (1)$$

In our investigation, we focus on measuring the dielectric function of $MAPbI_3$ and $MAPb_{1-x}Ge_x$ PbI_3 within the range of 200 to 1000 nm, as shown in Figure 5.

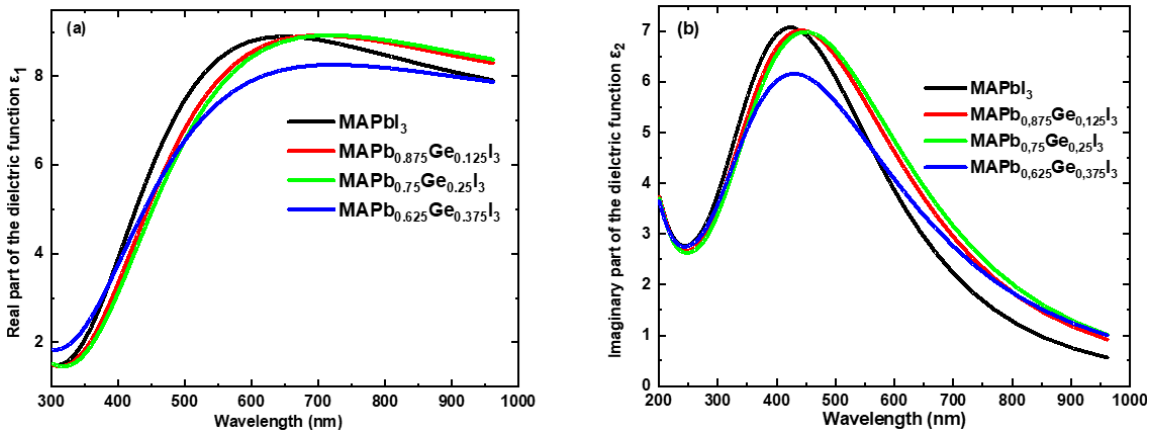

Fig. 5. Real component (a) and imaginary Component of dielectric function of $MAPbI_3$ and $MAPb_{1-x}$ Ge_x PbI_3 stucture (x = 0.125, 0.25, 0.375).

The real part $\varepsilon_1(\omega)$ exhibits two peaks for the pure MAPbI3 structure: the first at 209 nm and the second at 642 nm. In contrast, for the doped $MAPb_{1-x}Ge_x$ PbI_3 structures (with x = 0.125, 0.25, 0.375), each structure also shows two distinct peaks. The first peak is observed at 642 nm for all doped structures, while the second peaks appear at 670 nm, 700 nm, and 700 nm for the different germanium concentrations. The variation of $\varepsilon_1(\omega)$ with respect to λ indicates that $MAPbI_3$ and $MAPb_{1-x}Ge_x$ PbI_3 are dispersive media. After doping lead (Pb) with germanium (Ge) in the $MAPbI_3$ perovskite, I found that the imaginary part $\varepsilon_2(\omega)$ shows a single peak for both the pure $MAPbI_3$ structure and the doped $MAPb_{1-x}Ge_x$ PbI_3 structures (with x = 0.125, 0.25, 0.375). This

finding indicates that germanium doping enhances absorption in the visible range. The rise in $\varepsilon_2(\omega)$ suggests that germanium introduces new intermediate energy levels within the bandgap, which facilitates electronic transitions and improves the perovskite's ability to absorb visible light [23]. Consequently, doping with germanium optimizes absorption of light, offering benefits for optoelectronic applications like solar cells and photonic devices.

3.2.2. Refractive index

The complex refractive index, $n^*(\omega)$ is a parameter used to describe how light propagates through a material [24]. This index is typically expressed in a complex form to account for the material's dissipative properties. It can be represented as follows :

$$n^*(\omega) = n(\omega) + ik(\omega) \quad (2)$$

$$n(\omega) = \sqrt{\frac{\varepsilon_1(\omega)}{2} + \sqrt{\frac{(\varepsilon_1(\omega))^2 + (\varepsilon_2(\omega))^2}{2}}} \quad (3)$$

$$k(\omega) = \sqrt{\frac{\left(\varepsilon_1^2 + \varepsilon_2^2\right)^{\frac{1}{2}} - \varepsilon_1}{2}} \quad (4)$$

As the doping of Pb by Ge in $MAPbI_3$ perovskite increases, both the real $n(\omega)$ and imaginary $k(\omega)$ parts of $n^*(\omega)$ in the visible range rise due to alterations in the material's electronic structure, as illustrated in Figure 6. The introduction of Ge creates new energy levels and alters electronic interactions, leading to a higher density of states for electronic transitions. This results in increased polarization of the material, which raises the $n(\omega)$, while also enhancing absorption in the visible spectrum, thereby increasing the $k(\omega)$.

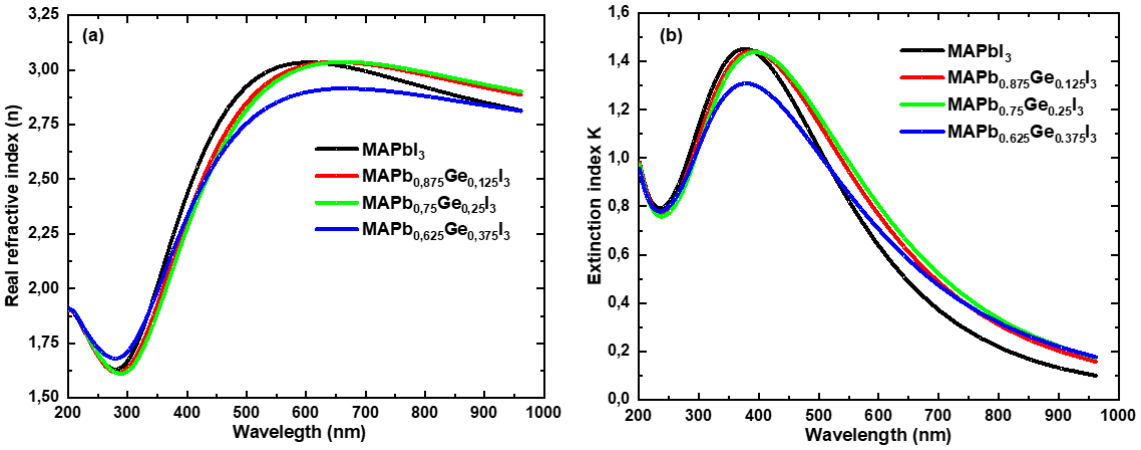

Fig. 6. Refractive index (a) and extinction index (b) of $MAPbI_3$ and its MAPb1-xGexI3 Structures.

3.2.3. Optical conductivity

Optical conductivity, denoted as σ, which is directly related to the $\varepsilon(\omega)$, characterizes the linear response of a material's charge carriers to an externally applied electromagnetic (EM) field. This optical conductivity is typically represented in the following form [25,26].

$$\sigma(\omega) = \sigma_1(\omega) + i\sigma_2(\omega) \quad (5)$$

$$\sigma_1(\omega) = 2nk\left(\frac{\omega}{4\pi}\right) \quad (6)$$

$$\sigma_2(\omega) = \left[1 - \left(n^2 - k^2\right)\right]\left(\frac{\omega}{4\pi}\right) \qquad (7)$$

Figure 7 shows the variation in optical conductivity for the materials $MAPbI_3$ and $MAPb_{1-x}Ge_xI_3$ within the range of 200 to 1000 nm. The MAPbI3 and $MAPb_{0.635}Ge_{0.375}I_3$ structures exhibit peaks with different intensities at 386 nm. In contrast, the $MAPb_{0.875}Ge_{0.125}I_3$ and $MAPb_{0.75}Ge_{0.25}I_3$ structures also display peaks with varying intensities at a wavelength of 406 nm. The peak value of real part of optical conductivity for the $MAPbI_3$ perovskite is 2.61 (1/fs). The σ_1 component of $MAPbI_3$ and doped structures reduces in the UV range and increases with the percentage of doping in the visible region, due to changes in light absorption by the material. The imaginary part, $\sigma_2(\omega)$, for $MAPbI_3$ and $MAPb_{1-x}Ge_xI_3$ exhibits negative values, with the minimum value reaching -2 (1/fs) at a wavelength of 500 nm.

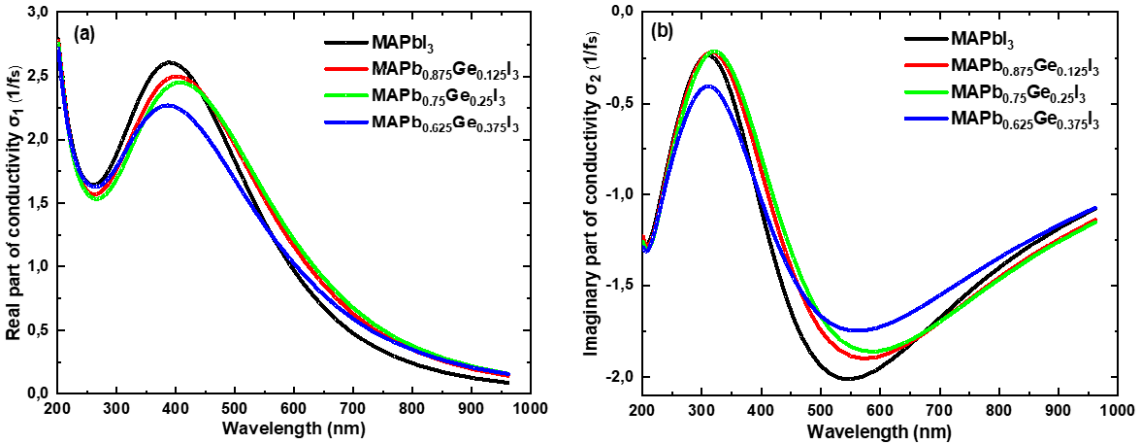

Fig.7. Real part (a) and the imaginary part (b) of the complex Optical conductivity, (b) imaginary part for the perovskite $MAPbI_3$ and its $MAPb_{1-x}Ge_xI_3$ as a function of wavelength.

3.2.4. Loss function

The optical loss function L(ω), determines the energy dissipated by incident photons as they propagate through a material. It can be expressed as [27-29].

$$L(\omega) = -Im\left(\frac{1}{\varepsilon(\omega)}\right) = \frac{\varepsilon_2(\omega)}{\varepsilon_1^2(\omega) + \varepsilon_2^2(\omega)} \qquad (8)$$

The variation of the function L(ω) for $MAPbI_3$ and $MAPb_{1-x}Ge_xI_3$ materials as a function of the incident wavelength as represented in Figure 8.

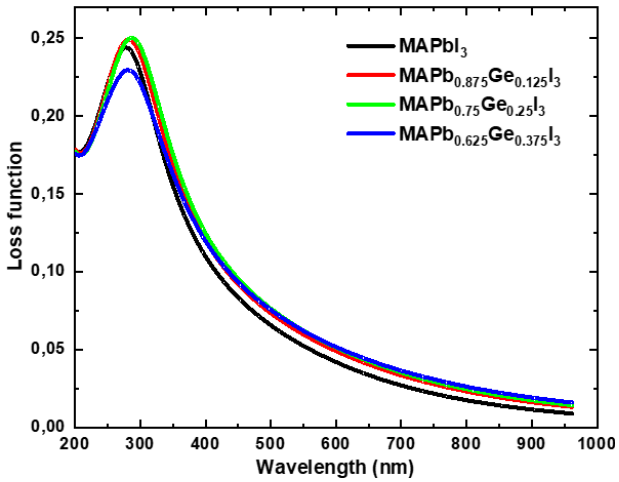

Fig. 8. Loss Function of $MAPb_{1-x}Ge_xI_3$ Structures (x = 0, 0.125, 0.25, 0.375) versus Wavelength.

The increase in Pb doping by Ge in $MAPbI_3$ perovskite results in a rise in the loss function L(ω) in the visible region of the spectrum. This effect is primarily due to the addition of novel energy states within the material's structure, which enhances the density of available electronic states for transitions. Additionally, changes in polarization and electronic interactions promote greater absorption of visible light. As a result, these combined factors lead to a significant increase in energy losses within the material.

4. CONCLUSION

We examined and analyzed in this research the electronic and optical features of $MAPbI_3$, as well as those of the $MAPb_{1-x}Ge_xI_3$ structure, where x denotes the germanium doping concentration. The investigation was conducted using first-principles calculations based on the DFT method. We employed the GGA+PBE approximation, as implemented in the CASTEP software. Doping $MAPbI_3$ with Ge at concentrations of 12.5%, 25%, and 37.5% led to a gradual reduction in bandgap energy and an an enhancement in the absorption coefficient within the visible spectrum. Additionally, Ge doping affected the overall TDOS, the components of $n^*(\omega)$, the $\varepsilon(\omega)$, $\sigma(\omega)$ and the L(ω). Doping $MAPbI_3$ with Ge enhances its optical and electronic properties by reducing the bandgap energy and improving absorption in the visible range, making it ideal for photovoltaic applications. These improvements open opportunities for its use in optoelectronic devices such as LEDs, as well as in laser systems and energy storage technologies.

Author Contributions: M. Lhouceine : Initial draft writing, software development, and investigation. A. Najim : Writing – original draft, Software, Investigation. A. Laassouli: Writing and Investigation. O. Bajjou: Supervision, Review and editing, Validation.K. Rahmani : Supervision, Review and editing. B. Manaut : Supervision, Review and validation.

Funding: No external funding was provided for this article.

Data availability Statement: Data will be made available upon inquiry.

Conflicts of Interest: The authors declare that they are not affiliated with any organization that has a direct or indirect financial interest in the subject matter discussed in this article.

Acknowledgments: The authors of this work would like to express their sincere gratitude to Sultan Moulay Slimane University and UNISA University.

REFERENCES

[1] S. Bilgen, "Structure and environmental impact of global energy consumption," Renewable and Sustainable Energy Reviews, vol. 38, pp. 890–902, Oct. 2014, doi: 10.1016/j.rser.2014.07.004.

[2] A. Shukla, V.K. Sharma, S.K. Gupta, A.S. Verma, "Computational determination of the physical-thermoelectric parameters of tin-based organomatallic halide perovskites (CH3NH3SnX3, X = Br and I): Emerging materials for optoelectronic devices". Materials Chemistry and Physics. 253, 123389 (2020). https://doi.org/10.1016/j.matchemphys.2020.123389

[3] A. Nicolas, J.-L. Barrat, J. Rottler, "Effects of inertia on the steady-shear rheology of disordered solids,". Phys. Rev. Lett. 116, 058303 (2016).

[4] L. Moulaoui, O. Bajjou, Y. Lachtioui, A. Najim, M. Archi, K. Rahmani, B. Manaut, "Modeling of Highly Efficient Lead Free MASnI3 Based Solar Cell with Graphene Oxide as Hole Transport Layer Using SCAPS 1D," . J. Electron. Mater. 52, 7541–7553 (2023). https://doi.org/10.1007/s11664-023-10684-4

[5] L. Moulaoui, A. Najim, A. Laassouli, M. Archi, A. Bakour, Y. Lachtioui, K. Rahmani, O. Bajjou, B. Manaut, "Theoretical investigations on the electronic and optical properties of Na-doped

CH3NH3PbI3 perovskite ''. E3S Web of Conferences.469, 00086 (2023). https://doi.org/10.1051/e3sconf/202346900086

[6] Bahadur, A. H. Ghahremani, S. Gupta, T. Druffel, M. K. Sunkara, K. Pal, ''Enhanced moisture stability of MAPbI3 perovskite solar cells through Barium doping". Solar Energy, 190, 396-404 (2019). https://doi.org/10.1016/j.solener.2019.08.033

[7] L. Qiu, S. He, J. Yang, F. Jin, J. Deng, H. Sun, X. Cheng, G. Guan, X. Sun, H. Zhaob, H. Peng, ''An all-solid-state fiber-type solar cell achieving 9.49% efficiency". J. Mater. Chem. A . 4, 10105 (2016). DOI: 10.1039/c6ta03263j

[8] J. Lu, S. Chen, H. Wang, L. Qiu, C. Wu, W. Qian, Z. Wang, K. Huang, J. Wu, H. Chen, and Y. Gao, "Replacing the electron-hole transport layer with doping: SCAPS simulation of lead-free germanium-based perovskite solar cells based on CsGeI3," Solar Energy Mater. Sol. Cells, vol. 271, p. 112883, Apr. 2024, doi: 10.1016/j.solmat.2024.112883.

[9] R. Chiara, M. Morana, and L. Malavasi, "Germanium-based halide perovskites: Materials, properties, and applications," ChemPlusChem, vol. 86, no. 8, pp. 879–888, 2021, doi: 10.1002/cplu.202100191.

[10] I. Diomandé, A. Bouich, A. A. Hyacinthe, B. M. Soucasse, and A. Boko, "Comparative Performance Analysis of MAPbI3 and FAPbI3 Perovskites: Study of Optoelectronic Properties and Stability," Modeling and Numerical Simulation of Material Science, vol. 13, no. 4, p. 134004, Oct. 2023, doi: 10.4236/mnsms.2023.134004.

[11] L. Moulaoui, O. Bajjou, A. Najim, K. Rahmani, A. Marouane, A. Laassouli, Y Lachtioui, B Manaut, ''Numerical Simulation of FAPbI3 perovskite based solar cells with graphene oxide as hole transport layer using SCAPS-1D", 2023 3rd International Conference on Innovative Research in Applied Science, Engineering and Technology (IRASET). https://doi.org/10.1109/IRASET57153.2023

[12] P. S.Whitfield, N. Herron, W. E.Guise, K. Page1, Y.Q. Cheng1, I. Milas and M. K. Crawford, ''Structures, Phase Transitions and Tricritical Behavior of the Hybrid Perovskite Methyl Ammonium Lead Iodide". Scientific Repots 6:35685 (2016). DOI: 10.1038/srep35685.

[13] K. Hossain, S. Khanom, F. Israt, M.K. Hossain, M.A. Hossain, F. Ahmed, First-principles study on structural, mechanical and optoelectronic properties of lead-free mixed Ge–Sn hybrid organic-inorganic perovskites. Solid State Communications. 320, 114024 (2020). https://doi.org/10.1016/j.ssc.2020.114024

[14] Y.Q. Huang, J. Su, Q.F. Li, D. Wang, L.H. Xu, Y. Bai, Structure, optical and electrical properties of $CH_3NH_3SnI_3$ single crystal. Physica B: Condensed Matter 563, 107–112 (2019). https://doi.org/10.1016/j.physb.2019.03.035.

[15] S.S. Bagade, M.M. Malik, P.K. Patel, The charm of entwining two major competitors CZTS and $CH_3NH_3SnI_3$ to feasibly explore photovoltaic world beyond Shockley–Queisser limit. Surfaces and Interfaces 46, 104020 (2024). https://doi.org/10.1016/j.surfin.2024.104020.

[16] K. Yan, B. Sun, T. Lu, X.D. Feng, Simulation of $MASnI_3$-based inverted perovskite solar cells with double hole transport layers and an electron transport layer. Optik 287, 171100 (2023). https://doi.org/10.1016/j.ijleo.2023.171100.

[17] J.H. Yoo, S.B. Kwon, J. Park, S.H. Choi, H.C. Yoo, B.K. Kang, Y.H. Song, S. Hong, D.H. Yoon, Potential usage of cesium manganese halide for multi-functional optoelectronic devices: Display & photodetector application. Chemical Engineering Journal 479, 147277 (2024). https://doi.org/10.1016/j.cej.2023.147277.

[18] J. Chang, G. Wang, Y. Huang, X. Luo, H. Chen, New insights into the electronic structures

and optical properties in the orthorhombic perovskite $MAPbI_3$: a mixture of Pb and Ge/Sn, New J. Chem. 41, 11413–11421 (2017). https://doi.org/10.1039/c7nj01442b.

[19] D. Liu, Q. Li, J. Hu, R. Sa, K. Wu, Photovoltaic Performance of Lead-Less Hybrid Perovskites from Theoretical Study. J. Phys. Chem. C 123, 12638–12646 (2019). https://doi.org/10.1021/acs.jpcc.9b02705.

[20] Y. Ogomi, A. Morita, S. Tsukamoto, T. Saitho, N. Fujikawa, Q. Shen, T. Toyoda, K. Yoshino, S.S. Pandey, T. Ma, S. Hayase, $CH_3NH_3Sn_xPb(1-_x)I_3$ Perovskite Solar Cells Covering up to 1060 nm. J. Phys. Chem. Lett. 5, 1004–1011 (2014). https://doi.org/10.1021/jz5002117.

[21] G. Niu, W. Li, J. Li, X. Liang, L. Wang, Enhancement of thermal stability for perovskite solar cells through cesium doping. RSC Advances 7, 17473–17479 (2017). https://doi.org/10.1039/C6RA28501E.

[22] H. Choi, J. Jeong, H.B. Kim, S. Kim, B. Walker, G.H. Kim, J.Y. Kim, Cesium-doped methylammonium lead iodide perovskite light absorber for hybrid solar cells. Nano Energy 7, 80–85 (2014). http://dx.doi.org/10.1016/j.nanoen.2014.04.017.

[23] S. Nations, T. Jia, S. Wang, Y. Duan, Electronic and optical properties of orthorhombic $(CH_3NH_3)BX_3$ (B = Sn, Pb; X = F, Cl, Br, I) perovskites: a first-principles investigation. RSC Adv. 11, 22264–22272 (2021). https://doi.org/10.1039/d1ra01586a.

[24] H. Arif, M.B. Tahir, M. Sagir, H. Alrobei, M. Alzaid, S. Ullah, M. Hussien, Effect of potassium on the structural, electronic, and optical properties of $CsSrF_3$ fluoro-perovskite: First-principles computation with GGA-PBE. Optik 259, 168741 (2022). https://doi.org/10.1016/j.ijleo.2022.168741.

[25] A. Taya, P. Rani, J. Thakur, M.K. Kashyap, First principles study of structural, electronic and optical properties of Cs-doped $CH_3NH_3PbI_3$ for photovoltaic applications. Vacuum 160, 440–444 (2019). https://doi.org/10.1016/j.vacuum.2018.12.008.

[26] L. Moulaoui, A. Najim, A. Laassouli, M. Archi, A. Bakour, Y. Lachtioui, K. Rahmani, O. Bajjou, B. Manaut, Theoretical investigations on the electronic and optical properties of Na-doped $CH_3NH_3PbI_3$ perovskite. E3S Web of Conferences 469, 00086 (2023). https://doi.org/10.1051/e3sconf/202346900086.

[27] A. Laassouli, O. Bajjou, Y. Lachtioui, A. Najim, L. Moulaoui, K. Rahmani, DFT investigation on the electronic and optical properties of Br-doped $CH_3NH_3SnI_3$ perovskite. 3rd International Conference on Innovative Research in Applied Science, Engineering and Technology (IRASET), Mohammedia, Morocco, May 18-19, June 21 (2023). https://doi.org/10.1109/IRASET57153.2023.10153066.

[28] A. Najim, O. Bajjou, L. Moulaoui, A. Laassouli, M. Archi, A. Bakour, Y. Lachtioui, K. Rahmani, Effects of lithium intercalation on the electronic and optical properties of graphene: Density Functional Theory (DFT) computing. 3rd International Conference on Innovative Research in Applied Science, Engineering and Technology (IRASET), Mohammedia, Morocco, May 18-19, June 21 (2023). https://doi.org/10.1109/IRASET57153.2023.10153044.

[29] A. Laassouli, L. Moulaoui, A. Najim, H. Errahoui, K. Rahmani, Y. Lachtioui, O. Bajjou, Phosphorus Doping Effects on the Optoelectronic Properties of $K_2AgAsBr_6$ Double Perovskites for Photovoltaic Applications. Solar Energy and Sustainable Development Journal, 14(SI_MSMS2E), 1–11 (2024). DOI:https://doi.org/10.51646/jsesd.v14iSI_MSMS2E.407.